Universal Journal of Green Chemistry
http://ojs.wiserpub.com/index.php/UJGC/

Research Article

Characterization and Disinfection Performance of α-Fe_2O_3-TiO_2 Based Polyester Membranes for Water Treatment

Zeinab A. Suliman[1,2*], Achisa C Mecha[3,4], Josphat I. Mwasiagi[1,5]

[1] Department of Manufacturing, Industrial and Textile Engineering, Moi University, Eldoret, Kenya
[2] Renewable Energy, Environment, Nanomaterials and Water Research Group, Department of Chemical Engineering and Technology, Gezira University, Wad Madani, Sudan
[3] Renewable Energy, Environment, Nanomaterials and Water Research Group, Department of Chemical and Process Engineering, Moi University, Eldoret, Kenya
[4] Department of Environmental Science, University of Arizona, Tucson, USA
[5] Departmeent of Technology Education, Open University of Kenya, Konza, Kenya
E-mail: zoba23165@gmail.com

Received: 8 October 2024; **Revised:** 18 November 2024; **Accepted:** 19 November 2024

Abstract: Water is essential for life; however, many people in developing countries, particularly in rural areas, lack access to clean and safe piped water. Lack of appropriate water treatment makes such people to consume untreated water containing biological and chemical pollutants, leading to diseases and even death. Hence, developing eco-friendly technologies using available resources can help address this critical issue. In this study α-Fe_2O_3-TiO_2 coated polyester membranes were employed the disinfection of water containing *Escherichia coli* (*E. coli*) as an indicator microorganism. The coated and uncoated membranes were characterized by scanning electron microscopy (SEM), energy-dispersive X-ray (EDX) spectroscopy, Fourier transform infrared spectroscopy (FTIR), X-ray diffraction (XRD). Antibacterial studies were done through direct contact with bacteria (glass bottle test) and the flow test under sunlight irradiation at various initial bacterial concentrations (2.45×10^3 to 2.45×10^5 CFU/mL). SEM images revealed the presence of the photocatalyst within the membranes, and EDX confirmed the successful impregnation through component analysis. A clear inhibition zone was observed around the coated membranes, 19 and 17 mm for 2.45×10^3 and 2.45×10^5 CFU/mL, respectively, and no inhibition zone was observed around the uncoated membranes. The coated membranes achieved disinfection efficiency of 91.3% in the glass bottle test and 98.30% in the flow test under sun light irradiation. The novelty of the study is that α-Fe_2O_3-TiO_2 impregnated photocatalytic membranes demonstrated excellent disinfection efficacy compared to the uncoated membranes and can readily be applied for water purification in areas that lack centralized water treatment systems.

Keywords: disinfection, α-Fe_2O_3-TiO_2 nanoparticles, *Escherichia coli*, polyester membrane, water treatment

1. Introduction

In recent years, numerous diseases have emerged, caused by various microbes such as bacteria, fungi, and viruses [1,2], which are transmitted by water[3], food[4], air[5], and even clothing[6]. Ensuring that drinking water is free from microbial contamination is critical, as even brief exposure can lead to waterborne illnesses. Consequently, regulations should emphasize the verification of drinking water's microbial safety. This is generally done by testing for indicator organisms,

Copyright ©2024 Zeinab A. Suliman, et al.
DOI: https://doi.org/10.37256/ujgc.2220245851
This is an open-access article distributed under a CC BY license
(Creative Commons Attribution 4.0 International License)
https://creativecommons.org/licenses/by/4.0/

with *Escherichia coli* (*E. coli*) being the preferred standard. *Thermotolerant coliforms* can also be used, though they are considered less reliable, yet still acceptable [7].

Traditional water treatment procedures are frequently employed to address bacterial pollution, especially in areas with low resources [8]. Boiling is one of the most basic and effective methods for killing germs and pathogens, as it include boiling water for at least one minute [9]. Another common method for disinfecting water is chlorination, which includes adding chlorine or sodium hypochlorite. It is frequently used in municipal and domestic water treatment because of its cost-effectiveness and capacity to destroy bacteria and viruses. However, it must be carefully regulated to avoid dangerous chemical consequences [10]. Filtration, using sand or ceramic filters, physically removes microorganisms from water. This technology traps impurities and is frequently combined with disinfection techniques such as chlorination to assure safety [11].

Membrane separation processes are widely used for water treatment to remove bacteria and other contaminants, providing an effective and sustainable solution. The most commonly used membrane technologies for bacterial removal are microfiltration (MF) and ultrafiltration (UF). Both processes rely on pressure gradients to push water through the membrane, while contaminants are retained on the surface or within the membrane structure. These techniques are chemical-free, making them environmentally friendly, and are widely used in drinking water treatment, wastewater management, and industrial applications. Membrane filtration is often combined with other disinfection methods, like chlorination or UV treatment, to ensure complete bacterial inactivation, providing a reliable, scalable, and energy-efficient way to achieve high water quality [12].

Nanoparticles, which range in size from 1–100 nm, effectively limit microbial growth, including Gram-positive and Gram-negative bacteria, as well as fungi. Their antibacterial effectiveness originates from their capacity to disrupt cell membranes, emit metal ions, and have inherent physical features. Metal-based nanoparticles, such as silver, copper, and zinc oxide and titanium dioxide, exhibit variable antibacterial activity [13–15].

Recent advances in nanomaterials have sparked interest in creating next-generation membranes with improved antifouling and anti-scaling capabilities for water and wastewater treatment. Key materials include silica, zeolites, metals (Ag, Zr, Ti), metal oxides (TiO_2, ZnO), metal-organic compounds, aquaporin proteins, and carbon-based materials such as graphene and carbon nanotubes [16,17]. Nanoparticles, particularly TiO_2, are added to membranes to boost photocatalytic capabilities for pollutant breakdown and disinfection. TiO_2's effectiveness in heterogeneous photocatalysis is affected by pollutant concentration and light intensity. Nanocomposites are utilised extensively in wastewater treatment, medicine delivery, and environmental cleanup [18–20].

Doping TiO_2 with ferric oxide (Fe_2O_3) has become a focus in photocatalytic research due to its ability to improve sunlight absorption and overall photocatalytic efficiency [21]. While TiO_2 is well-regarded for its stability and photocatalytic properties, its effectiveness is hindered by limited light absorption, confined to the UV spectrum below 400 nm, corresponding to wide band-gap energy of 3.76 eV. This restriction reduces its capability under sunlight, as the UV portion makes up only a minor part of the solar spectrum. In comparison, α-Fe_2O_3 (hematite) exhibits broader absorption within the UV–visible range and shows photo-absorption near 527 nm, with smaller band-gap energy of 2.35 eV. Integrating α-Fe_2O_3 into TiO_2 forms α-Fe_2O_3-TiO_2 composite materials that extend the optical absorption range and shift absorption into the visible light region. This red-shift is due to the α-Fe_2O_3 component, enabling better sunlight utilization for photocatalysis. Notably, α-Fe_2O_3-doped TiO_2 composites exhibit absorption around 438.8 nm, corresponding to band-gap energy of 2.83 eV. This enhanced light absorption makes α-Fe_2O_3-TiO_2 composites attractive for solar-driven applications, including environmental cleanup and the degradation of organic pollutants in water [22].

Photocatalytic membranes, which combine physical filtration with photocatalytic degradation using materials like titanium dioxide (TiO_2), Fe_2O_3 doped TiO_2, and solar-powered treatment systems, reduce dependency on conventional energy sources. These technologies have a synergistic impact in that the combination of photocatalysis and filtration improves not only the disinfection performance but also the overall efficiency of contaminant removal. Furthermore, the photocatalytic action aids in the reduction of membrane fouling by decomposing organic foulants on the membrane surface, increasing the membrane's lifespan and reuse [16,17,23].

In this study α-Fe_2O_3-TiO_2 was incorporated into polyester membranes using an *ex-situ* method to obtain an integrated photocatalytic membrane with superior disinfection efficacy. Doping the titanium dioxide with ferric oxide enhanced the capacity to absorb visible light thus enabling the use of natural sun light to activate the photocatalyst and facilitate the

inactivation of bacteria. The novelty of the study is that α-Fe_2O_3-TiO_2 impregnated photocatalytic membranes can be applied as standalone water purification systems in areas that lack centralized water treatment systems. The use of natural sunlight and gravity based flow eliminates the need for UV lamps and pumps, thereby making the process economical and environmentally friendly.

2. Materials and methods

2.1 *Materials*

Titanium dioxide (TiO_2) powder and iron (III) nitrate nonahydrate (Fe $(NO_3)_3 \cdot 9H_2O$) supplied by DLA company, Isopropanol ($(CH_3)_2CHOH$, supplied by Gelsup company, absolute ethanol (C_2H_5OH) (supplied by Eldo lab), and polyethylene terephthalate (PET) polyester fabric membranes; (65% polyester, 35% cotton) supplied by Rift valley textiles (Rivatex) Ltd. All the chemical reagents employed in this study were of analytical grade, necessitating no additional purification.

2.2 *Impregnation of the photocatalysts into the polyester membranes*

The α-Fe_2O_3-TiO_2 was integrated into polyester membranes using an ex-situ method. The α-Fe_2O_3-TiO_2 was synthesized from $Fe(NO_3)_3 \cdot 9H_2O$ and commercial TiO_2, as detailed in our previous approach[22]. A solution of iron (III) nitrate (0.6 M) was prepared by dissolving iron (III) nitrate nonahydrate ($Fe(NO_3)_3 \cdot 9H_2O$) in ethanol. Titanium dioxide (TiO_2) powder was added to the solution, which was stirred magnetically while sealed to prevent ethanol evaporation. After 30 min of stirring, the mixture was sonicated, first for 15 min at 35 kHz, followed by 15 min at 130 kHz. The cover was then removed, and the ethanol was evaporated overnight at 50 °C on a hot plate. The dried product was calcined for 10 min at 300 °C, ground into a powder, and heated in a furnace for 6 h at 300 °C.

The immobilization of α-Fe_2O_3-TiO_2 nanoparticles onto polyester membranes was performed using a modified aqueous heat attachment method, based on the protocol by[24] first; polyester membranes (40 cm × 40 cm) were thoroughly cleaned with detergent at 80 °C for 30 min to remove impurities. They were then rinsed with water to remove detergent residues and treated with acetone at 25 °C for 30 min. Next, the membranes were immersed in a 1 M NaOH solution at 80 °C for 5 h, followed by thorough rinsing with water and drying at 80 °C for 24 h.

Once cleaned, the membranes were immersed in α-Fe_2O_3-TiO_2 suspension at 80 °C for 2 h while stirred magnetically at 200 rpm, and then dried at 40 °C for 24 h. This immersion and drying cycle was repeated three times. The α-Fe_2O_3-TiO_2 concentration was adjusted to achieve a coating density of 8 g/m^2 on the membranes. Afterward, the coated membranes were cured at 150 °C for 30 min, followed by immersion in water at 80 °C for 30 min to remove loosely bound particles. Finally, they were dried at 80 °C for 24 h and stored in a desiccator for future use.

2.3 *Characterization of the photocatalysts*

The α-Fe_2O_3-TiO_2 photocatalysts were synthesized and reported in our previous study[22]. The α-Fe_2O_3-TiO_2 coated polyester membranes were characterized for surface morphology through scanning electron microscopy (SEM: Zeiss, Ultra55). The chemical composition was analyzed through Fourier transform infrared spectroscopy (FTIR: PerkinElmer, Frontier) in ATR mode, covering a range of 4000–650 cm^{-1}. X-ray diffraction (XRD) analysis, performed with a Smartlab X-ray Diffractometer capable of PXRD, HRXRD, and XRR, was used to determine the structure of the coated membranes. Additionally, chemical characterization was performed using energy-dispersive X-ray (EDX) spectroscopy.

2.4 *The disinfection performance of the photocatalysts coated membranes*

The antibacterial efficacy of both coated and uncoated membranes (used as controls) was evaluated against gram-negative *Escherichia coli* (*E. coli*) strain ATCC 25922. This was done through contact of the membranes with *E. coli* containing media, employing qualitative techniques Disk Diffusion and Glass Bottle tests. Additionally, the disinfection

efficiency of the coated membrane was assessed during the filtration of water with varying *E. coli* concentrations (Flow test).

A concentrated bacterial culture was diluted using a serial dilution method. Initially, 1 gram of concentrated bacteria was dissolved in 9 mL of distilled water to achieve a concentration of 10^0 bacteria. After thorough mixing, 1 mL of this solution was further diluted with 9 mL of water to achieve a concentration of 10^1 bacteria. This process was repeated until reaching a concentration of 10^6 bacteria. Figure 1 illustrates the shaking process and the bacterial concentrations ranging from 10^0 to 10^6 CFU/mL

(a) b

Figure 1. Bacteria dilution (**a**) shaker and (**b**) the bacteria concentrations (10^0–10^6) CFU/mL

2.4.1 *Disk diffusion test*

In the disk diffusion test, coated and uncoated membrane pieces were placed on MacConkey agar plates pre-inoculated with *E. coli*, serving as controls. The antibacterial compounds from the membranes diffuse into the agar, forming a gradient. If the compound inhibits bacterial growth, a clear inhibition zone forms around the membrane, indicating antibacterial activity. MacConkey agar (51.5 g/L) was prepared, and all materials were autoclaved. *E. coli* at concentrations of 2.45 $\times$ 10^5 CFU/mL and 2.45 $\times$ 10^3 CFU/mL were applied to the agar. The membranes were incubated for 24 h at 37 °C, and inhibition zones were measured.

2.4.2 *Glass bottle test*

The Glass Bottle Test evaluates the disinfection efficacy of a substance in liquid containing target microorganisms. In this method, the substance is submerged in the liquid, allowing its antimicrobial properties to diffuse and inhibit microbial growth. For this study, 0.1 mL of *E. coli* (98,000 CFU/mL) was added to a glass bottle and diluted to 10 mL. Coated and uncoated membrane pieces (10 $\times$ 10 mm) were then introduced into the bottle, mixed, and 0.1 mL of the solution was transferred onto agar media for analysis. The percentage reduction in bacterial colonies (R%) was calculated using Equation (1)

$$R\% = \left(\frac{A-B}{A}\right) * 100 \quad (1)$$

where, A and B represent the number of bacteria colonies in CFU for uncoated and coated membranes, respectively.

2.4.3 *Flow test*

To prepare synthetic bacterial feeds, 1 mL of the 10^6 CFU/mL solutions was diluted to 10 mL, and then 0.1 mL was transferred to 10 liters to create a feed with 12×10^4 CFU/100 mL (high concentration). This feed was filtered under solar irradiation for 90 min, with samples collected every 30 min, using various coated membranes and an uncoated membrane control. A medium (6×10^4 CFU/100 mL) concentration of synthetic feed and low (13×10^3 CFU/100) concentration real water feed from dam also tested for antimicrobial efficiency. Bacterial growth was evaluated on MacConkey agar, and disinfection efficacy was calculated using log removal values (LRV) to compare influent and effluent bacterial counts.

$$LRV = \log_{10}(C_f/C_p) \tag{2}$$

where C_f and C_p represent the concentrations of microorganisms in the influent and effluent, respectively.

3. Results and discussion

3.1 *Characterization of the photocatalysts*

The characterization of bare TiO_2, α-Fe_2O_3 photocatalysts, and co-doped α-Fe_2O_3-TiO_2 composites was performed as detailed in our previous work[22]. SEM imaging confirmed the presence of the photocatalytic nanoparticles, while FTIR and XRD analyses revealed distinct peaks associated with these materials. UV-DRS analysis showed that doping TiO_2 with α-Fe_2O_3 enhanced its band-gap properties and shifted the absorption into the visible light spectrum, facilitating improved sunlight absorption.

3.2 *Characterization of the photocatalysts*

3.2.1 *SEM & EDX analysis*

Figure 2 shows SEM images of the coated and uncoated membrane surfaces at magnifications of 100.00 kX and 75.00 kX. In images (a) and (b), the coated membrane surface displays the presence of a material, presumed to be α-Fe_2O_3-TiO_2 nanoparticles (NPs). The micrographs reveal a porous and clustered morphology, suggesting enhancements in surface properties. Both large and small particles of similar size were observed. When compared to the uncoated membranes, the coated ones exhibited a smoother surface, indicating that the photocatalyst improved the membrane's texture, making it softer than its uncoated counterpart. The α-Fe_2O_3-TiO_2-coated polyester-cotton membrane likely exhibited a smoother texture due to the uniform distribution of the photocatalyst on its surface. The nanoparticles form a thin, even coating that fills in surface irregularities, enhancing the membrane's overall smoothness. This coating can also create stronger binding interactions between the α-Fe_2O_3-TiO_2 particles and the membrane fibers, resulting in better adhesion and structural cohesion. Additionally, any heat treatment involved during preparation can facilitate integration and densification, further refining the surface. The presence of α-Fe_2O_3-TiO_2 may also promote a reorganization of the polyester-cotton matrix, reducing micro-defects and creating a more even and uniform surface.

The EDX analysis of the coated membranes, shown in Figure 3, highlights the chemical composition. The spectrum revealed distinct peaks, indicating the presence of 0.33% Ti, 46.53% O, 52.9% C, and 0.25% Fe in the coated membrane. These elemental results confirm that only the fabric membrane and photocatalyst materials are present, demonstrating the high purity and effectiveness of the impregnation process.

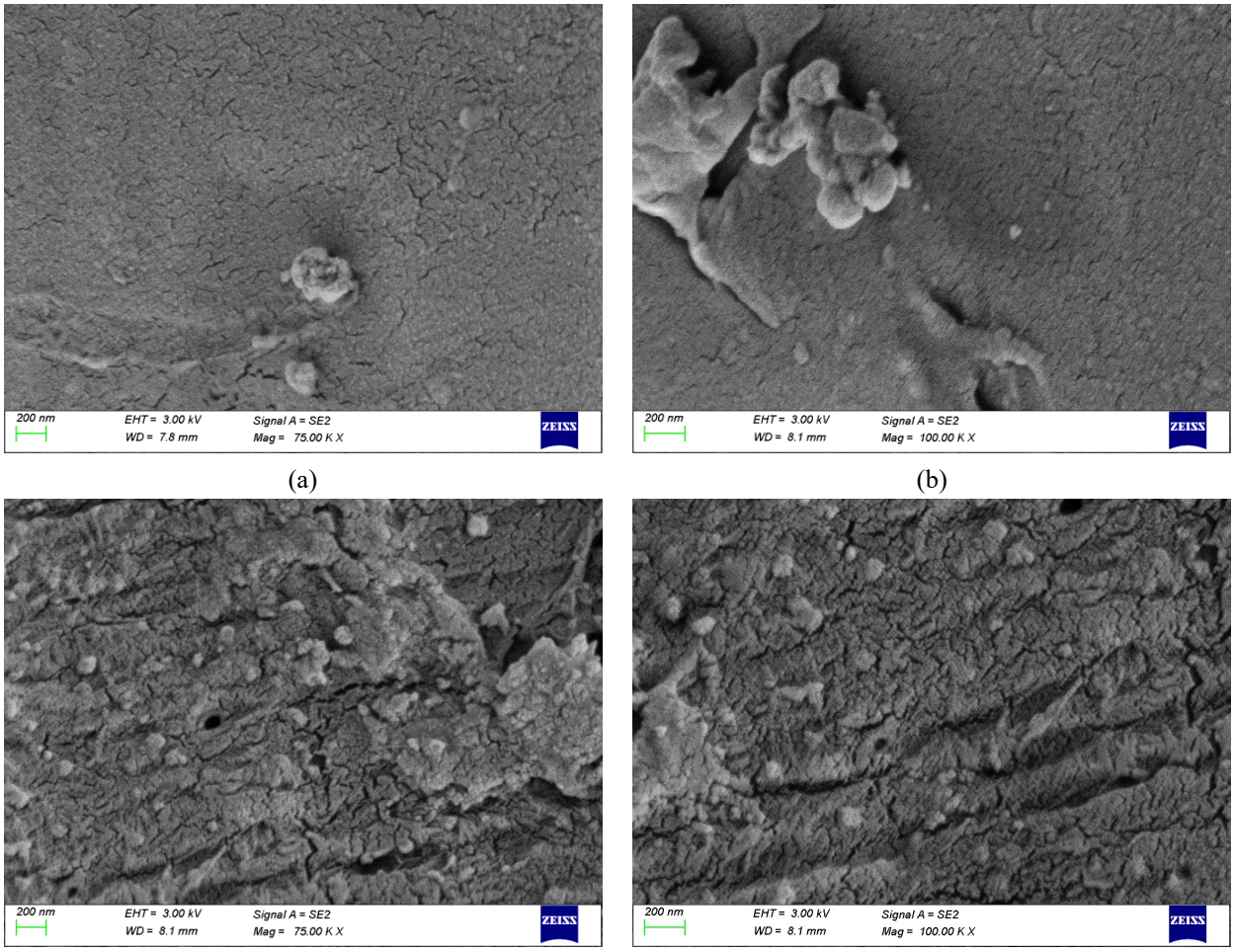

Figure 2. SEM images of (**a**,**b**) coated membranes and (**c**,**d**) uncoated membranes (control) at 100 k× and 75 k× magnifications

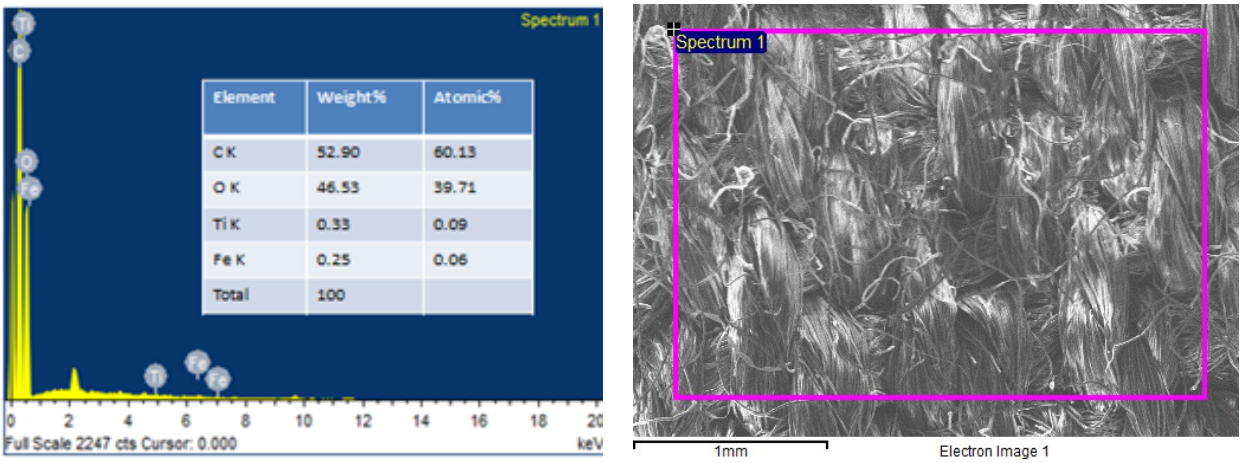

Figure 3. EDX images of the coated membranes showing the chemical composition

3.2.2 *FTIR analysis*

FTIR analysis (Figure 4) was performed on both uncoated and coated polyester-cotton membranes, identifying the characteristic functional groups of the fabric materials. Prominent peaks at 1162 cm^{-1} and 1709 cm^{-1} confirmed the membranes' polyester-dominant composition[25], while the cotton component exhibited distinct absorption bands, including C=O stretching, C–O stretching, and O-H deformation within the 1200–1700 cm^{-1} range. A broad absorption band between 3600 and 3000 cm^{-1} was linked to OH stretching and hydrogen bonding in the cellulose structure, alongside peaks for methylene and methine stretching observed in the 3000–2800 cm^{-1} range[26]. Despite the introduction of α-Fe_2O_3-TiO_2 nanoparticles, no significant shifts in the FTIR peaks were observed between coated and uncoated membranes. This lack of variation is likely due to the low nanoparticle concentration and minimal chemical bonding, aligning with previous studies on nanoparticle-coated textiles[27]. The peak reductions in coated membranes are attributed to reactions between the membranes and the photocatalyst.

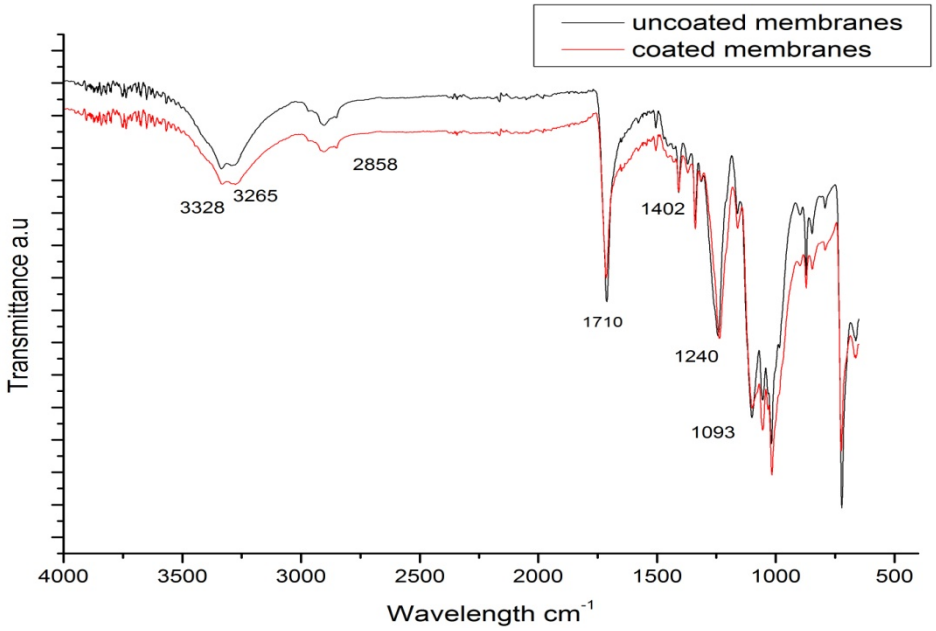

Figure 4. FTIR curves of coated and uncoated membranes

3.2.3 *XRD analysis*

Figure 5 presents the XRD patterns of both coated and uncoated membranes, highlighting the distinct crystalline structures of the polyester-cotton blend. The diffraction pattern for cotton reveals prominent peaks at 2θ values of 14.5, 22.7[28], 33.96 and 45.4[29] while the polyester exhibits notable peaks at 2θ values of 16.5, 22.6, and 25.2[28]. The diffraction peaks observed in both treated and untreated membranes reflect the fabric's inherent semi-crystalline nature, indicating that the surface treatment does not disrupt the original crystalline structure. This consistency suggests that the modification applied is heterogeneous and does not alter the fabric's molecular arrangement or crystallinity[30,31]. The observed shift in peaks, particularly at 33.96 and between 25.2 and 14.5, is attributed to the interaction between the membranes and the photocatalyst.

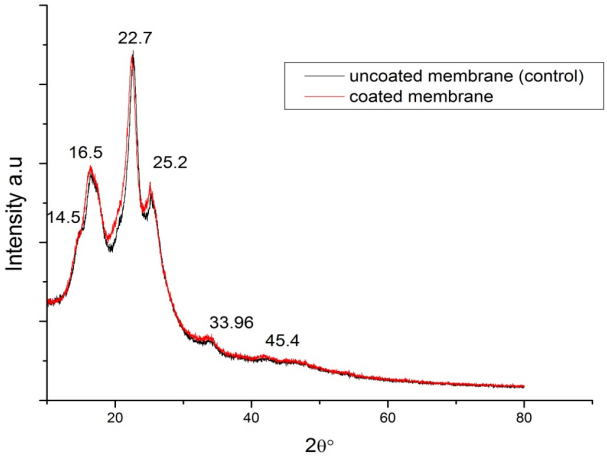

Figure 5. XRD patterns of coated and uncoated membranes

3.3 *The disinfection performance of the photocatalysts coated membranes*

3.3.1 *Disk diffusion*

Table 1 displays the zone of inhibition (in millimeters) for coated membranes, as well as uncoated membranes, against negative bacteria (*E. coli*) using concentrations of 2.45×10^5 and 2.45×10^3 CFU/mL.

In Figure 6, the growth of the inhibition zone is clearly depicted for *E. coli* concentration 2.45×10^5 CFU/mL for both coated and uncoated membranes. Notably, around the uncoated membranes, bacterial growth is observed everywhere, even on the membrane itself, indicating the absence of antimicrobial properties in plain polyester. Conversely, for coated membranes, clear inhibition zones are evident around each, varying in length depending on the bacteria concentration. Using a lighter concentration of bacteria, 2.45×10^3 CFU/mL concentrations expand the inhibition zone for coated membranes due to the reduction in bacterial numbers. However, the uncoated membranes still lack an inhibition zone due to their absence of antimicrobial properties.

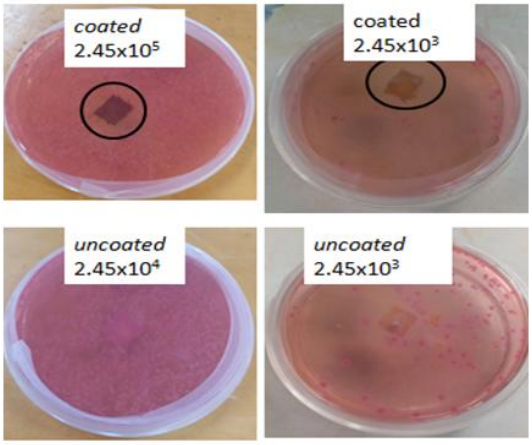

Figure 6. Zone of inhibition in mm for the coated and uncoated membranes against *E. coli* (2.45×10^5 and 2.45×10^3) CFU/mL concentration

Table 1. Zone of inhibition in mm for the coated and uncoated membranes against *E. coli* (2.45×10^5 and 2.45×10^3) CFU/mL concentration

Membranes type	Zone of inhibition in mm *E. coli*	
	2.45×10^5 CFU/mL	2.45×10^3 CFU/mL
Uncoated membrane	Zero	zero
coated membrane	17	19

The generation of reactive oxygen species, such as superoxides and hydroxyl radicals, which penetrate bacterial cells and damage their membranes, is what gives photocatalyst nanoparticles their antibacterial characteristics [32]. The incorporation of TiO_2 doped with ferric oxide into polyester fabric enables the inactivation of gram-negative bacteria such as *E. coli,* Prorokova et al. incorporated photocatalysts of titanium dioxide doped with ferric into polyester fabric and observed inhibition zones when testing the antimicrobial properties of the coated fabric against *E. coli* [33].

3.3.2 *Glass bottle test*

Table 2 elucidates the removal efficiency of *E. coli* 9.8×10^5 CFU/100 mL concentration using membranes coated with α-Fe_2O_3-TiO_2 as well as the uncoated membrane, as determined through the glass bottle test method. The results confirm that the uncoated membranes lack antimicrobial activity, resulting in a zero-removal efficiency of *E. coli*. The coated membranes exhibited antimicrobial efficiency of 91.3%. This effectiveness stems from the combined action of both photocatalysts, TiO_2 [34] and Fe_2O_3 [35]. Indeed, both doping photocatalysts contributed to the overall antimicrobial function of the membranes.

Table 2. Removal efficiency of *E. coli* using the Glass bottle test

Membranes type	*E. coli* removal efficiency %
Uncoated membrane	0.00
coated membrane	91.30

3.3.3 *The flow test*

The disinfection efficiency of three different feed concentrations of water was evaluated. The concentrations were as follows: high (12×10^4 CFU/100 mL), medium (6×10^4 CFU/100 mL) for synthetic feed water and low concentration 13×10^3 CFU/100 mL of real feed water. The removal efficiency (%) and Log Reduction Value (LRV) were calculated and are presented in Table 3.

Table 3. Disinfection efficacy of the synthetic feed water

Membranes type	Synthetic feed (*E. Coli*)				Dam water (*E. Coli*)	
	12×10^4 CFU/100 mL		6×10^4 CFU/100 mL		13×10^3 CFU/100 mL	
	Removal %	LRV	Removal %	LRV	Removal %	LRV
Uncoated	64.60	0.45	63.50	0.44	65.00	0.46
Coated	98.00	1.70	97.50	1.60	98.30	1.77

For the synthetic feed, the uncoated filters achieved notable *E. coli* removal percentages of 64.6% and 63.5% for the high and medium *E. coli* concentrations, respectively. The corresponding Log Reduction Values (LRVs) were 0.45 for the high concentration and 0.44 for the medium concentration. This indicates that the removal efficiency improved as the *E. coli* concentration in the feed water increased. The likely reason for this is that higher concentrations caused more *E. coli* to deposit on the filter surface, enhancing the filtration effectiveness [36]. The removal efficiency of the dam water increased to 65%, and the Log Reduction Value (LRV) became 0.46. This improvement in removal efficiency may be attributed to the lower initial concentration of *E. coli*, which can lead to more effective filtration process. Additionally, the

natural turbidity of the dam water might have helped reduce the effective pore size of the membranes, thereby enhancing the removal efficiency.

For the membranes coated with titanium dioxide doping with ferric oxide, there was an increase in removal percentage and Log Reduction Value (LRV) due to the antimicrobial properties of the TiO_2 [37,38] and Fe_2O_3 [39,40] photocatalysts. The removal percentages achieved were 98% for high concentrations, 97.50% for medium concentrations, and 98.30% for dam water concentrations. The corresponding LRVs were 1.70 for high concentrations, 1.60 for medium concentrations, and 1.77 for dam water concentrations.

4. Conclusions

The red coloration confirmed the successful incorporation of α-Fe_2O_3-TiO_2 into polyester membranes, as further validated by characterization results. SEM images revealed the presence of the photocatalyst within the membrane structure, while EDX confirmed successful impregnation by detecting its elemental composition. On the other hand, both FTIR and XRD analyses indicated the presence of polyester/cotton fabric in both coated and uncoated membranes. This confirms that the membranes maintain their polyester/cotton composition after coating, ensuring structural consistency throughout the process. Coated membranes exhibited strong antibacterial activity, with inhibition zones of 17 and 19 mm, while uncoated membranes allowed bacterial growth, including on the surface, demonstrating the photocatalyst's effectiveness. Flow tests showed enhanced disinfection efficiency, with Log Reduction Values (LVR) increasing from 0.45, 0.44, and 0.46 for uncoated membranes to 1.7, 1.6, and 1.77 for coated membranes under high, medium, and low bacterial concentrations, respectively. The study, conducted with high bacterial concentrations, yielded effective results, suggesting the coated membranes would perform even more efficiently in real water systems with typically lower bacterial levels.

Conflict of interest

The authors declare no conflict of interest.

References

[1] Baker, R. E.; Mahmud, A. S.; Miller, I. F.; Rajeev, M.; Rasambainarivo, F.; Rice, B. L.; Takahashi, S.; Tatem, A. J.; Wagner, C. E.; Wang, L.-F. Infectious Disease in an Era of Global Change. *Nat. Rev. Microbiol.* **2022**, *20*, 193–205.

[2] Chen, B.; Jiang, Y.; Cao, X.; Liu, C.; Zhang, N.; Shi, D. Droplet Digital PCR as an Emerging Tool in Detecting Pathogens Nucleic Acids in Infectious Diseases. *Clin. Chim. Acta* **2021**, *517*, 156–161.

[3] World Health Organization. *Guidelines for Drinking-Water Quality: Incorporating the First and Second Addenda*; World Health Organization: Geneva, Switzerland, 2022.

[4] Dawson, P. Transfer of Microorganisms and Respiratory Viruses through Food. *Med. Res. Arch.* **2020**, *8*. https://doi.org/10.18103/mra.v8i5.2105.

[5] Šantl-Temkiv, T.; Amato, P.; Casamayor, E. O.; Lee, P. K.; Pointing, S. B. Microbial Ecology of the Atmosphere. *FEMS Microbiol. Rev.* **2022**, *46*, fuac009.

[6] Mirzaei, M.; Furxhi, I.; Murphy, F.; Mullins, M. A Supervised Machine-Learning Prediction of Textile's Antimicrobial Capacity Coated with Nanomaterials. *Coatings* **2021**, *11*, 1532.

[7] World Health Organization. *Guidelines for Drinking-Water Quality: Small Water Supplies*; World Health Organization: Geneva, Switzerland, 2024.

[8] Saravanan, A.; Kumar, P. S.; Jeevanantham, S.; Karishma, S.; Tajsabreen, B.; Yaashikaa, P.; Reshma, B. Effective Water/Wastewater Treatment Methodologies for Toxic Pollutants Removal: Processes and Applications towards Sustainable Development. *Chemosphere* **2021**, *280*, 130595.

[9] Manzoor, A.; Jan, B.; Zahoor, I.; Anjum, N.; Nabi, A.; Allai, F. M.; Rizvi, Q. U. E. H.; Shiekh, R. A.; Sheikh, M. A.; Ahmad, S. Thermal Treatment of Foods: Science, Shelf Life, and Quality. In *Shelf Life Food Safety*; CRC Press: Boca Raton, FL, USA, 2022; pp 165–180.

[10] Srivastav, A. L.; Patel, N.; Chaudhary, V. K. Disinfection By-Products in Drinking Water: Occurrence, Toxicity and Abatement. *Environ. Pollut.* **2020**, *267*, 115474.
[11] Abdiyev, K.; Azat, S.; Kuldeyev, E.; Ybyraiymkul, D.; Kabdrakhmanova, S.; Berndtsson, R.; Khalkhabai, B.; Kabdrakhmanova, A.; Sultakhan, S. Review of Slow Sand Filtration for Raw Water Treatment with Potential Application in Less-Developed Countries. *Water* **2023**, *15*, 2007.
[12] Chhabra, R. P.; Gurappa, B. *Coulson and Richardson's Chemical Engineering*, 2A; Butterworth-Heinemann: Waltham, MA, USA, 2019.
[13] Biswal, A. K.; Misra, P. K. Biosynthesis and Characterization of Silver Nanoparticles for Prospective Application in Food Packaging and Biomedical Fields. *Molecules* **2020**, *250*, 123014.
[14] Correa, M. G.; Martínez, F. B.; Vidal, C. P.; Streitt, C.; Escrig, J.; de Dicastillo, C. L. Antimicrobial Metal-Based Nanoparticles: A Review on Their Synthesis, Types and Antimicrobial Action. *Beilstein J. Nanotechnol.* **2020**, *11*, 1450–1469.
[15] Song, X.; Bayati, P.; Gupta, M.; Elahinia, M.; Haghshenas, M. Fracture of Magnesium Matrix Nanocomposites–A Review. *Int. J. Lightweight Mater. Manuf.* **2021**, *4*, 67–98.
[16] Anand, A.; Unnikrishnan, B.; Mao, J.-Y.; Lin, H.-J.; Huang, C.-C. Graphene-Based Nanofiltration Membranes for Improving Salt Rejection, Water Flux and Antifouling–A Review. *Desalination* **2018**, *429*, 119–133.
[17] Bodzek, M.; Konieczny, K.; Kwiecińska-Mydlak, A. Application of Nanotechnology and Nanomaterials in Water and Wastewater Treatment: Membranes, Photocatalysis and Disinfection. *Desalination Water Treat.* **2020**, *186*, 88–106.
[18] Bouziane Errahmani, K.; Benhabiles, O.; Bellebia, S.; Bengharez, Z.; Goosen, M.; Mahmoudi, H. Photocatalytic Nanocomposite Polymer-TiO_2 Membranes for Pollutant Removal from Wastewater. *Catalysts* **2021**, *11*, 402.
[19] Ghafourian, N.; Hosseini, S. N.; Mahmoodi, Z.; Masnabadi, N.; Thalji, M. R.; Abhari, A. R.; Al Zoubi, W.; Chong, K. F.; Ali, G. A.; Bakr, Z. H. TiO_2-Mica 450 Composite for Photocatalytic Degradation of Methylene Blue Using UV Irradiation. *Emergent Mater.* **2023**, *6*, 1527–1536.
[20] Naseem, T.; Waseem, M. A Comprehensive Review on the Role of Some Important Nanocomposites for Antimicrobial and Wastewater Applications. *Int. J. Environ. Sci. Technol.* **2022**, *19*, 2221–2246.
[21] Rafiq, K.; Asghar, S.; Abid, M. Z.; Sultana, M.; Waleed, M. Z.; Hashem, A.; Avila-Quezada, G. D.; Abd_Allah, E. F.; Hussain, E. Unveiling the Potential of Fe_2O_3/TiO_2 System to Produce Clean Water: An Effective and Low-Cost Approach for Arsenic Removal from Ground Water. *Surfaces Interfaces* **2024**, *52*, 104913.
[22] Suliman, Z. A.; Mecha, A. C.; Mwasiagi, J. I. Effect of TiO_2/Fe_2O_3 Nanopowder Synthesis Method on Visible Light Photocatalytic Degradation of Reactive Blue Dye. *Heliyon* **2024**, *10*, 8e29648.
[23] Song, N.; Gao, X.; Ma, Z.; Wang, X.; Wei, Y.; Gao, C. A Review of Graphene-Based Separation Membrane: Materials, Characteristics, Preparation and Applications. *Desalination* **2018**, *437*, 59–72.
[24] Sudrajat, H. J. Superior Photocatalytic Activity of Polyester Fabrics Coated with Zinc Oxide from Waste Hot Dipping Zinc. *J. Cleaner Prod.* **2018**, *172*, 1722–1729.
[25] Agrawal, N.; Low, P. S.; Tan, J. S. J.; Fong, E. W. M.; Lai, Y.; Chen, Z. Durable Easy-Cleaning and Antibacterial Cotton Fabrics Using Fluorine-Free Silane Coupling Agents and CuO Nanoparticles. *Nano Mater. Sci.* **2020**, *2*, 281–291.
[26] Alosmanov, R.; Buniyat-Zadeh, I.; Soylak, M.; Shukurov, A.; Aliyeva, S.; Turp, S.; Guliyeva, G. Design, Structural Characteristic and Antibacterial Performance of Silver-Containing Cotton Fiber Nanocomposite. *Bioengineering* **2022**, *9*, 770.
[27] Mecha, C. A.; Pillay, V. L. Development and Evaluation of Woven Fabric Microfiltration Membranes Impregnated with Silver Nanoparticles for Potable Water Treatment. *J. Membr. Sci.* **2014**, *458*, 149–156.
[28] Muthukumar, N.; Thilagavathi, G. Development and Characterization of Electrically Conductive Polyaniline Coated Fabrics. *Indian J. Chem. Technol.* **2012**, *19*, 434–441.
[29] Al-Khattaf, F.; Al Mousa, A.; Alabdulhadi, H.; Abo-Dahab, N.; Mohamed, H.; Hatamleh, A.; Al-Dahmash, N. Characterization and Antibacterial Activity of Raw Cotton Fabrics Treated with Date Seed Extract and Silver Nanoparticles (AgNPs). *Braz. J. Biol.* **2023**, *83*, e270217.
[30] Dong, W.; Zhou, M.; Li, Y.; Zhai, S.; Jin, K.; Fan, Z.; Zhao, H.; Zou, W.; Cai, Z. Low-Salt Dyeing of Cotton Fabric Grafted with pH-Responsive Cationic Polymer of Polyelectrolyte 2-(N,N-Dimethylamino) Ethyl Methacrylate. *Colloids Surf. A: Physicochem. Eng. Aspects* **2020**, *594*, 124573.
[31] El-Naggar, H.; Abd Al-Halim, M.; Gaballa, A. S.; Hassouba, M. Surface Improvement of Cotton/Polyester Blend Textile Using DC Air Glow Discharge Plasma. *PhyS* **2021**, *96*, 125712.

[32] Parra-Ortiz, E.; Malmsten, M. Photocatalytic Nanoparticles–From Membrane Interactions to Antimicrobial and Antiviral Effects. *Adv. Colloid Interface Sci.* **2022**, *299*, 102526.
[33] Prorokova, N.; Kumeeva, T.; Kholodkov, I. Formation of Coatings Based on Titanium Dioxide Nanosolson Polyester Fibre Materials. *Coatings* **2020**, *10*, 82.
[34] Zhang, G.; Wang, D.; Yan, J.; Xiao, Y.; Gu, W.; Zang, C. Study on the Photocatalytic and Antibacterial Properties of TiO_2 Nanoparticles-Coated Cotton Fabrics. *Materials* **2019**, *12*, 2010.
[35] Granados, A.; Pleixats, R.; Vallribera, A. Recent Advances on Antimicrobial and Anti-Inflammatory Cotton Fabrics Containing Nanostructures. *Molecules* **2021**, *26*, 3008.
[36] Achisa, C. M. Evaluation of Silver Nanoparticles Impregnated Woven Fabric Microfiltration Membranes for Potable Water Treatment. Ph.D. Thesis, Durban University of Technology, Durban, South Africa, 2014.
[37] Chand, K.; Cao, D.; Fouad, D. E.; Shah, A. H.; Lakhan, M. N.; Dayo, A. Q.; Sagar, H. J.; Zhu, K.; Mohamed, A. M. A. Photocatalytic and Antimicrobial Activity of Biosynthesized Silver and Titanium Dioxide Nanoparticles: A Comparative Study. *J. Mol. Liq.* **2020**, *316*, 113821.
[38] Khashan, K. S.; Sulaiman, G. M.; Abdulameer, F. A.; Albukhaty, S.; Ibrahem, M. A.; Al-Muhimeed, T.; AlObaid, A. A. Antibacterial Activity of TiO_2 Nanoparticles Prepared by One-Step Laser Ablation in Liquid. *Appl. Sci.* **2021**, *11*, 4623.
[39] Zúñiga-Miranda, J.; Guerra, J.; Mueller, A.; Mayorga-Ramos, A.; Carrera-Pacheco, S. E.; Barba-Ostria, C.; Heredia-Moya, J.; Guamán, L. P. Iron Oxide Nanoparticles: Green Synthesis and Their Antimicrobial Activity. *Nanomaterials* **2023**, *13*, 2919.
[40] Ezealigo, U. S.; Ezealigo, B. N.; Aisida, S. O.; Ezema, F. I. Iron Oxide Nanoparticles: Synthesis, Characterization, and Applications. *Nanomaterials* **2023**.